Pharmaceutical Research, Vol. 6, No. 2, 1989

Research Article

Statistical Moment Analysis of Hepatobiliary Transport of Phenol Red in the Perfused Rat Liver

Koyo Nishida,[1] Chiaki Tonegawa,[1] Toshiyuki Kakutani,[1] Mitsuru Hashida,[1] and Hitoshi Sezaki[1,2]

Received April 18, 1988; accepted September 25, 1988

A new experimental system was applied to study hepatobiliary transport of drugs. Rat livers were perfused using a single-pass technique, and phenol red was momentarily introduced to this system from the portal side. Outflow dilution patterns of phenol red were analyzed using statistical moment theory, and kinetic parameters of hepatic distribution and elimination of phenol red were calculated from moments, namely, the hepatic extraction ratio (E_i) and elimination rate constant ($k_{el,i}$). A larger distribution volume (V_i) was obtained for phenol red than for ^{131}I-human serum albumin (HSA) and ^{51}Cr-red blood cells (RBC), indicating its extravascular diffusivity. The biliary excretion of conjugated phenol red was delayed relative to that of the free agent. The larger biliary mean transit time ($\bar{t}_{bile,conj.}$) represents the processes of biliary transport and intrahepatic metabolism. Further, the effects of dose and perfusion temperature on the hepatobiliary transport of phenol red were determined. With high doses or low perfusion temperatures (20 and 27°C), E_i, $k_{el,i}$, and intrinsic clearance ($CL_{int,i}$) of phenol red and biliary recovery of free and conjugated phenol red ($F_{bile,free}$, $F_{bile,conj.}$) significantly decreased. The temperature-dependent and saturable processes in hepatic uptake, metabolism, and biliary excretion of phenol red were assessable to moment analysis.

KEY WORDS: phenol red; rat liver perfusion; hepatic uptake; metabolism; biliary excretion; moment analysis.

INTRODUCTION

The hepatobiliary transport system plays an important role in drug disposition in the body. Many investigators have attempted to quantify the individual transfer processes of drug from the blood to the bile. However, the individual transport processes are usually not evaluated by means of a single experimental system. We have developed an experimental system in which statistical moment analysis was adopted for a local organ perfusion experiment (1). An advantage of this approach is the ability to assess drug disposition quantitatively by dividing it into distribution and elimination aspects. Therefore, this theory should be useful to characterize the hepatobiliary transport and metabolism mechanism of drugs.

In this paper, single-pass rat liver perfusion experiments were carried out to investigate the hepatobiliary transport system of phenol red. Phenol red shows the typical characteristics of organic anions including carrier-mediated transport in sinusoidal and/or bile-canalicular membranes of hepatocytes, protein binding in cytosol, and conjugative metabolism. Therefore, phenol red is a suitable model for testing the ability of an analytical approach to resolve many simultaneous hepatobiliary transport processes. Phenol red was momentarily injected from the portal side to the perfused liver and its outflow dilution and biliary excretion were analyzed by statistical moment theory.

MATERIALS AND METHODS

Animals. Male Wistar rats (190–210 g) with free access to standard rat foods and water were used.

Chemicals. Phenol red was purchased from Nakarai Chemicals Co., Kyoto, Japan. ^{131}I-Human serum albumin (HSA) (1 mCi/ml) was purchased from Daiichi Radioisotopes, Tokyo. $Na_2[^{51}Cr]O_4$ (0.5 mCi/mg) was obtained from New England Nuclear, Boston, Mass. All other chemicals were of reagent grade and were obtained commercially from Nakarai Chemicals Co., Kyoto, Japan. Red blood cells (RBC) were labeled by incubating with $Na_2[^{51}Cr]O_4$ at 37°C for 20 min followed by repeated washing with Krebs–Ringer bicarbonate buffer.

Liver Perfusions. Rat liver was perfused *in situ* as described by Mortimore *et al.* (2) with slight modifications. Rats were anesthetized with pentobarbital (60 mg/kg i.p.) and the common bile duct was cannulated with a polyethylene tube (PE-10). The portal vein was rapidly catheterized with a polyethylene tube (PE-160), which was attached to the perfusate of Krebs–Ringer bicarbonate buffer with 10 m*M* glucose (oxygenated with 95% O_2–5% CO_2 to pH 7.4 at

[1] Department of Basic Pharmaceutics, Faculty of Pharmaceutical Sciences, Kyoto University, Sakyo-ku, Kyoto 606, Japan.
[2] To whom correspondence should be addressed at Faculty of Pharmaceutical Sciences, Kyoto University, Sakyo-ku, Kyoto 606, Japan.

0724-8741/89/0200-0140$06.00/0

37°C), and infusion of the perfusate was started immediately. The inferior vena cava was catheterized through the right atrium with a polyethylene tube (PE-160) and then was ligated right above the renal vein. The perfusate was circulated using a peristaltic pump (SJ-1211, ATTO Co., Tokyo) at a flow rate of 12.65 ± 0.48 ml/min (mean ± SD). The experiments at low temperature were carried out with the perfusate maintained at 20 or 27°C. To avoid the effect of interaction with albumin and simplify the perfusion system, liver perfusion was carried out with albumin-free perfusate.

After a stabilization period of 30 min, phenol red dissolving in the perfusion medium (0.1328 ml) was introduced into the portal vein using a six-position rotary valve injector (Type 50 Teflon rotary valves, Rheodyne, Cotati, Calif.). The time period over which the pulse dose was given corresponded to 0.63 sec in the perfusate flow. Venous outflow samples were collected into the previously weighed tube at 1- to 3-sec intervals for 1 min. The sampling interval was 1 sec at first and was gradually prolonged. The sample volumes collected were calculated from the gain in weight in the tube assuming the density of the outflowing perfusate to be 1.0. The sampling time point was calculated from each sample volume assuming a constant flow rate.

Bile samples were collected into the weighed small test tubes at adequate time intervals for 60 min. The sampling interval was 3 min at first and was gradually prolonged. The bile sample volumes collected were calculated as described for the venous outflow samples. The sampling time was taken as the midpoint time during the sampling period. After the perfusion experiment, the whole liver was excised and weighed. The mean weight of the liver was 8.44 ±1.17 g.

The time courses of the dilution curves were corrected for the lag time due to the internal volumes of catheters (total, ca. 0.64 ml). The viability of the liver was checked by the bile flow (>4 μl/min) and the serum glutamic oxaloacetic transaminase activity in the hepatic venous outflow (<10 Karmen units). In all experiments, perfused rat livers remained viable during the course of the study. ^{131}I-HSA and ^{51}Cr-RBC were used as the extracellular reference substance and vascular reference substance, respectively.

Assay. The concentration of free phenol red in the effluent perfusate and bile sample was determined spectrophotometrically at 560 nm after dilution with a 1 *N* NaOH solution. The total concentration of free and conjugated phenol red was measured in the same manner after they were subjected to acid hydrolysis (1 *N* HCl at 100°C for 30 min) (3). The concentration of conjugated phenol red was estimated from the difference between these values. The radioactivities of ^{131}I and ^{51}Cr in the outflow sample were counted with a gamma counter (ARC-500, Aloka Co., Tokyo).

Pharmacokinetic Analysis of Outflow Patterns and Biliary Excretion Patterns. The theoretical background of data analysis was given previously (1). For the comprehension of the pharmacokinetic parameters derived from this analysis, several points are stressed.

(a) The equations presented are derived based on the physiological one-organ model, denoting by the subscript i. The circulatory system is observed as a black box under linear disposition conditions, and the disposition function of the system is reflected in the outflow pattern to a unit pulse input. The statistical moment analysis was originally introduced into pharmacokinetics by Yamaoka *et al.* (4) and Cutler (5) for *in vivo* systems. It has been applied to a single-pass organ perfusion system, by reducing the outflow pattern into statistical moments.

(b) The first three (zeroth to second) moments for the outflow pattern are defined as follows:

$$\text{auc}_i = \int_0^\infty C\,dt \tag{1}$$

$$t_i = \int_0^\infty t \cdot C\,dt/\text{auc}_i \tag{2}$$

$$\sigma_i^2 = \int_0^\infty (t - \bar{t}_i)^2 \cdot C\,dt/\text{auc}_i \tag{3}$$

where t is the time, C is the concentration of substances normalized by the injection dose as the percentage of the dose per milliliter, and auc_i, $\bar{t}_i$, and σ_i^2 are the area under the concentration–time curve, the mean transit time, and the variance of transit time, respectively. The moments are calculated by numeral integration using a linear trapezoidal formula and extrapolation to infinite time based on a monoexponential equation (1,4). The $\bar{t}_i$ and σ_i^2 values were corrected for the lag time of the catheter and its variation.

(c) By the application of the chromatographic concepts and the well-stirred model (6–9), the disposition parameters to assess the local drug disposition are derived from the moments. The derivation methods of the disposition parameters are summarized in Table 1. They can be divided into two groups, that is, parameters representing distribution (V_i, $\bar{t}_{cor,i}$, and k_i) and those representing elimination (E_i, F_i, $k_{el,i}$, and $CL_{int,i}$).

The hepatic flow rate (Q_i) is expressed as milliliters per second per gram of liver and the experimentally obtained value for each run was used. E_i and F_i depend on the experimental condition (e.g., liver weight and flow rate) as well as the first three moments. Other parameters are independent of the hepatic flow rate. V_i and $CL_{int,i}$ are expressed as milliliters per gram of liver and milliliters per minute per gram of liver, respectively.

(d) The biliary excretion rate–time curves of free and conjugated phenol red were analyzed independently based on statistical moment theory.

Moments are defined as follows:

$$F_{\text{bile,free}} = \int_0^\infty (dXb_{\text{free}}/dt)dt \tag{12}$$

$$F_{\text{bile,conj.}} = \int_0^\infty (dXb_{\text{conj.}}/dt)dt \tag{13}$$

$$\bar{t}_{\text{bile,free}} = \int_0^\infty t \cdot (dXb_{\text{free}}/dt)dt/F_{\text{bile,free}} \tag{14}$$

$$\bar{t}_{\text{bile,conj.}} = \int_0^\infty t \cdot (dXb_{\text{conj.}}/dt)dt/F_{\text{bile,conj.}} \tag{15}$$

where t is the time, and dXb_{free}/dt and $dXb_{\text{conj.}}/dt$ are the biliary excretion rates of free and conjugated phenol red, respectively. The values of dXb_{free}/dt and $dXb_{\text{conj.}}/dt$ are normalized with the injected dose and expressed as the percentage of the dose per minute. $F_{\text{bile,free}}$ and $F_{\text{bile,conj.}}$ are the biliary recovery ratios of free and conjugated phenol red, respectively. $\bar{t}_{\text{bile,free}}$ and $\bar{t}_{\text{bile,conj.}}$ are the biliary mean tran-

Table I. Derivation of the Disposition Parameters from Moments

(a)	Distribution		
	Extent		
	Distribution volume[a]	$V_i = Q_i \cdot \bar{t}_i/F_i$	(4)
	Tissue distribution ratio[b]	$k_i = (\bar{t}_i/F_i)/\bar{t}_B - 1$	(5)
	Corrected mean transit time	$\bar{t}_{cor,i} = \bar{t}_i/F_i$	(6)
(b)	Elimination		
	Extent		
	Recovery ratio	$F_i = auc_i \cdot Q$	(7)
	Extraction ratio	$E_i = 1 - F_i$	(8)
	Rate		
	Mean elimination time	$\bar{t}_{el,i} = \bar{t}_i/E_i$	(9)
	First-order elimination rate constant	$k_{el,i} = E_i/\bar{t}_i$	(10)
(c)	Clearance	$CL_{int,i} = k_{el,i} \cdot V_i$	(11)
	Intrinsic clearance		

[a] The value of Q_i measured in each run was employed for calculation.
[b] $\bar{t}_B$ is the mean transit time of ^{131}I-HSA.

sit times of free and conjugated phenol red, respectively. The moments are calculated by numeral integration using a linear trapezoidal formula and extrapolation to infinite time based on a monoexponential equation, from the excretion rate–time curves.

RESULTS

Liver Perfusion of Vascular Reference Substances and Phenol Red

Figure 1 illustrates typical outflow concentration–time curves of ^{51}Cr-RBC, ^{131}I-HSA, and phenol red (dose, 1.33 mg/liver). The outflow pattern of phenol red showed a diminution in peak concentration in comparison with those of ^{51}Cr-RBC and ^{131}I-HSA. Test substances could not be detected after the end point of sampling (1 min) and conjugated phenol red could not be detected in the outflow sample during sampling period.

Moments and disposition parameters for these results are summarized in Table II. The V_i values for ^{51}Cr-RBC and ^{131}I-HSA, which correspond to the volume of the sinusoidal space and sinusoidal space plus the space of Disse, respectively, were calculated to be 0.209 and 0.252 ml/g liver in this experimental system. These values were comparable to those obtained by Stollman *et al.* (10). Phenol red exhibited a larger V_i (0.310 ml/g liver) than did ^{131}I-HSA (0.252 ml/g liver), suggesting its extravascular distribution. E_i and $k_{el,i}$ values of phenol red would reflect its hepatic uptake and metabolic degradation.

Effect of Dose

In Fig. 2, typical outflow concentration–time curves of phenol red at doses of 0.133, 1.33, and 4.00 mg/liver are compared. The normalized peak concentration decreased as the injection dose decreased. The calculated moments and disposition parameters of phenol red at these doses are also

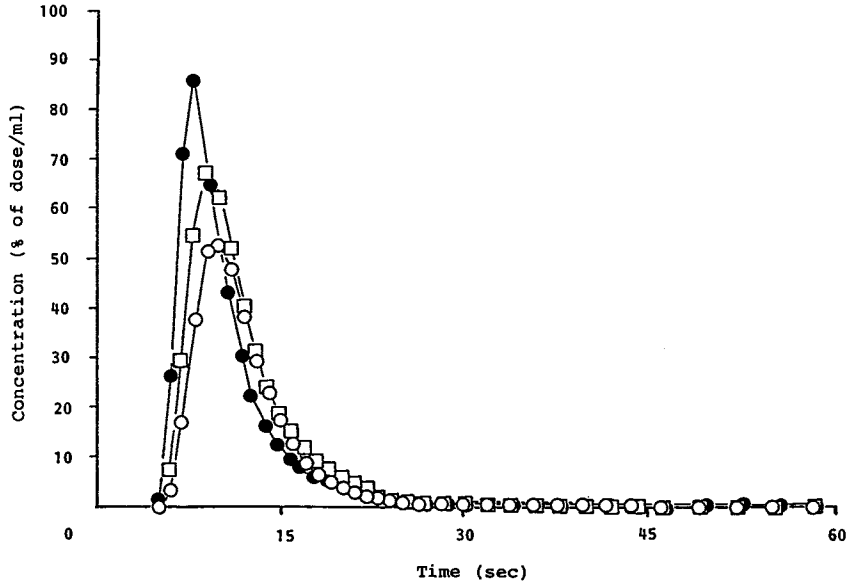

Fig. 1. Typical outflow patterns of ^{51}Cr-RBC (●), ^{131}I-HSA (□), and phenol red (○) in the single-pass rat liver perfusion system. The dose of phenol red was 1.33 mg/liver.

Table II. Moments and Representative Disposition Parameters for ^{51}Cr-RBC, ^{131}I-HSA, and Phenol Red in the Single-Pass Rat Liver Perfusion System (Values Are Means ± SD)

	Moment parameter			Disposition parameter			
				Distribution,	Elimination		Clearance,
	auc_i (% of dose · sec/ml)	$\bar{t}_i$ (sec)	σ_i^2 (sec^2)	extent, V_i (ml/g liver)	Extent, E_i (%)	Rate, $k_{el,i}$ (min^{-1})	$CL_{int,i}$ (ml/min/g liver)
^{51}Cr-RBC	471.3 ± 24.5	8.89 ± 0.83	42.1 ± 14.3	0.209 ± 0.013	0	—	0
^{131}I-HSA	485.9 ± 14.3	9.33 ± 1.09	36.8 ± 17.5	0.252 ± 0.051	0	—	0
Phenol red							
Standard dose (1.33 mg/liver)	389.7 ± 14.4	9.86 ± 1.37	28.1 ± 2.7	0.310 ± 0.068	17.77 ± 3.81	1.094 ± 0.279	0.332 ± 0.080
High dose (4.00 mg/liver)	458.8 ± 9.8*	9.91 ± 1.05	29.1 ± 6.0	0.253 ± 0.021	4.20 ± 2.22*	0.251 ± 0.117*	0.065 ± 0.036*
Low dose (0.133 mg/liver)	279.5 ± 20.8*	10.14 ± 1.31	58.5 ± 7.8*	0.376 ± 0.110	40.14 ± 3.06*	2.384 ± 0.197*	0.887 ± 0.199*

* $P < 0.05$ in comparison with phenol red (standard dose, 1.33 mg/liver).

summarized in Table II. E_i, $k_{el,i}$, and $CL_{int,i}$ values remarkably decreased with an increase in injection dose. This indicated that the elimination process of phenol red has been saturated at the high-dose area, at least in part. V_i values also decreased as the injection dose increased.

Effect of Perfusion Temperature

Figure 3 shows typical outflow concentration–time curves of phenol red at 20, 27, and 37°C. The outflow patterns at 20 and 27°C showed a concomitant delay in the time of transit in comparison with that at 37°C (standard experimental condition). Moments and disposition parameters of phenol red at various perfusion temperatures are summarized in Table III. E_i, $k_{el,i}$, and $CL_{int,i}$ values decreased as the perfusion temperature was lowered. These findings should correlate with the active transport of phenol red from the bloodstream into the hepatocyte and/or metabolism. On the other hand, V_i values increased as the perfusion temperature was lowered.

In the same way, outflow concentration–time curves of ^{131}I-HSA at 20, 27, and 37°C are compared in Fig. 4. The moments and disposition parameters calculated from these results are also listed in Table III. V_i values of ^{131}I-HSA at 20 and 27°C significantly decreased in comparison with that obtained at 37°C, similar to the results for phenol red. This indicated that hepatic hemodynamics changed to have a larger vascular space at low perfusion temperatures in this perfusion system.

Biliary Excretion of Free and Conjugated Phenol Red

Figure 5 illustrates typical biliary excretion rate–time curves of free and conjugated phenol red under the standard experimental condition (dose of 1.33 mg/liver and 37°C). The biliary excretion rate–time curves of conjugated phenol red

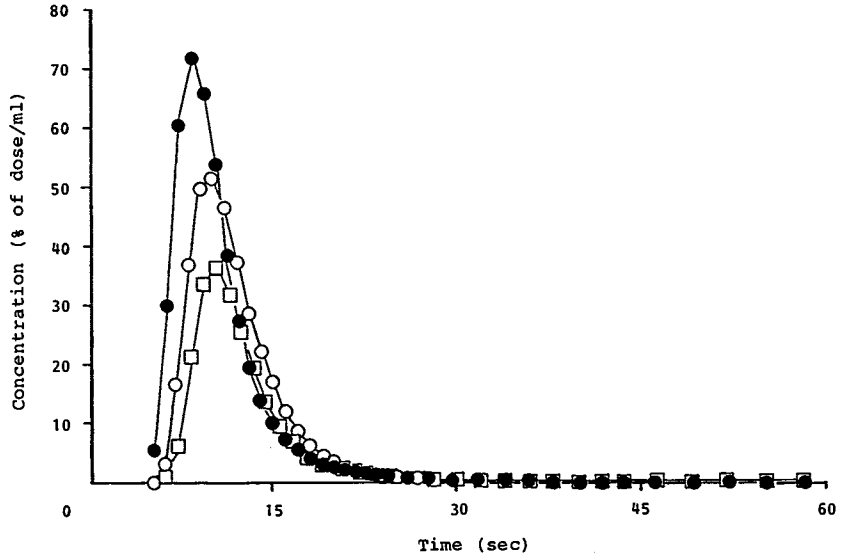

Fig. 2. Outflow patterns of phenol red at a dose of 0.133 mg/liver (□), 1.33 mg/liver (○), and 4.00 mg/liver (●) in the single-pass rat liver perfusion system.

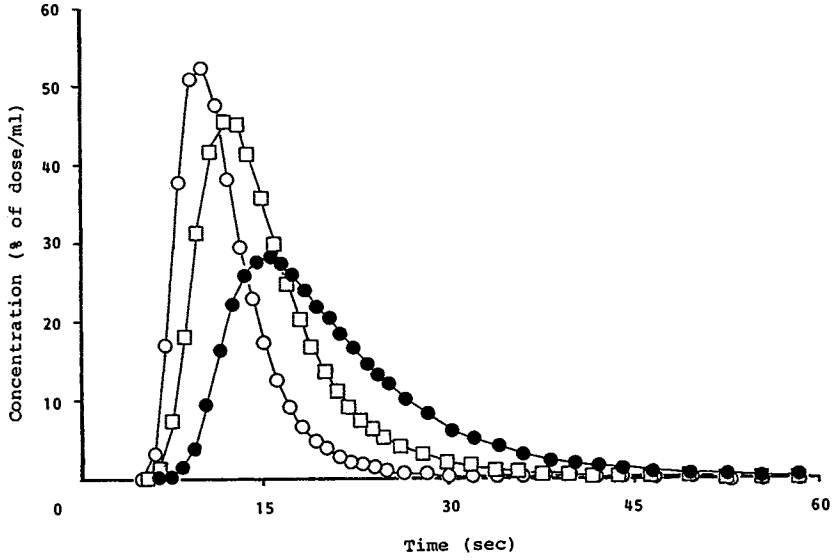

Fig. 3. Outflow patterns of phenol red (dose, 1.33 mg/liver) in the single-pass rat liver perfusion system at 20°C (●), 27°C (□), and 37°C (○).

showed a delay in the biliary appearance in comparison with that of free phenol red. Similar results were obtained in the case of the low perfusion temperature (27°C) and high dose (4.00 mg/liver). Moments for biliary excretion of free and conjugated phenol red are summarized in Table IV. The $\bar{t}_{bile,free}$ values were significantly lower than the $\bar{t}_{bile,conj.}$ values under all experimental conditions. The ratio of $F_{bile,conj.}$ to $F_{bile,free}$ decreased in the cases of low temperature and high dose, suggesting the suppression of metabolic process under these conditions.

DISCUSSION

The objective of this work is the assessment of a new method for analysis of hepatobiliary transport of drugs in which statistical moment theory is applied to a single-pass rat liver perfusion system.

The isolated liver perfusion is a valuable and commonly used tool for exploring the physiology and pathophysiology of the liver. In contrast to *in vivo* models, the isolated perfused liver permits reliable exposure of the hepatocytes to test substances under various but well-defined conditions. Furthermore, experiments can be done independently of the influence of other organ systems, plasma constituents, and neural–hormonal effects. Compared with *in vitro* models, on the other hand, hepatic architecture, cell polarity, and bile formation capacity are preserved in the liver perfusion system.

In the perfusion system, hepatobiliary transport of drugs can be studied in several administration models, i.e., the recirculation method (11,12), constant infusion method (13,14), and single-pass bolus injection method (15,16). In the field of physiology, the indicator dilution method, i.e., bolus injection modality, is often employed since it enables

Table III. Moments and Representative Disposition Parameters for Phenol Red[a] and ^{131}I-HSA in the Single-Pass Rat Liver Perfusion System at 37, 27, and 20°C (Values Are Means ± SD)

	Moment parameter			Disposition parameter			
				Distribution,	Elimination		Clearance,
	auc_i (% of dose · sec/ml)	$\bar{t}_i$ (sec)	σ_i^2 (sec^2)	extent, V_i (ml/g liver)	Extent, E_i (%)	Rate, $k_{el,i}$ (min^{-1})	$CL_{int,i}$ (ml/min/g liver)
37°C							
Phenol red	389.7 ± 14.4	9.86 ± 1.37	28.1 ± 2.7	0.310 ± 0.068	17.77 ± 3.81	1.094 ± 0.279	0.332 ± 0.080
^{131}I-HSA	485.9 ± 14.3	9.33 ± 1.09	36.8 ± 17.5	0.252 ± 0.051	0	—	0
27°C							
Phenol red	443.7 ± 10.8*	12.91 ± 1.86*	34.9 ± 5.0*	0.388 ± 0.023*	7.91 ± 3.20*	0.385 ± 0.200*	0.147 ± 0.071*
^{131}I-HSA	479.4 ± 10.7	12.64 ± 1.15*	39.0 ± 11.4	0.306 ± 0.046	0	—	0
20°C							
Phenol red	437.8 ± 18.6*	18.61 ± 2.29*	57.8 ± 15.2*	0.430 ± 0.062*	6.62 ± 4.43*	0.202 ± 0.120*	0.092 ± 0.062*
^{131}I-HSA	474.7 ± 15.4	15.97 ± 1.11*	47.1 ± 4.7*	0.393 ± 0.052*	0	—	0

[a] The dose of phenol red was 1.33 mg/liver (standard dose).

* $P < 0.05$ in comparison with the parameters for phenol red and ^{131}I-HSA at 37°C, respectively.

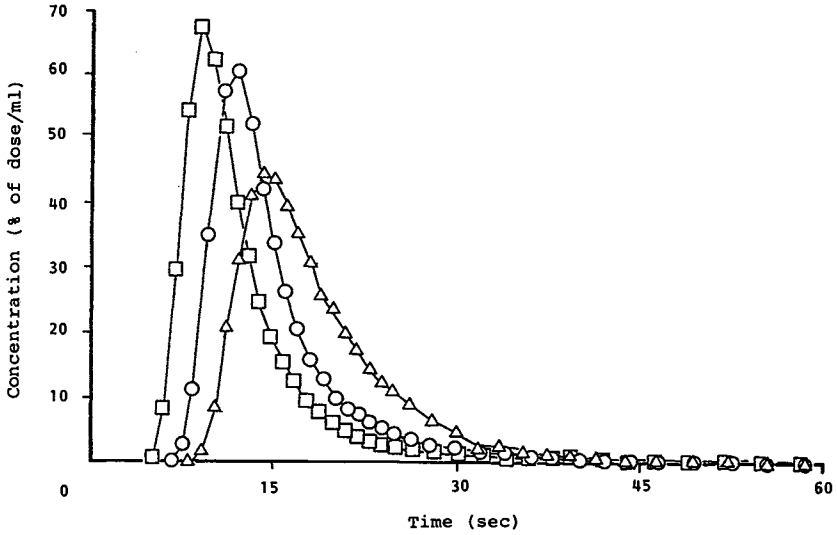

Fig. 4. Outflow patterns of ^{131}I-HSA in the single-pass rat liver perfusion system at 20°C (△), 27°C (○), and 37°C (□).

us to analyze the various dynamic processes in hepatobiliary transport of drugs in combination with a complex model (17). However, such models may be more sophisticated than is warranted by the experimental data (18–20). Complex deterministic models (17,21–23) are certainly valid in limited situations but lack general applicability.

In our approach, a simple well-stirred model (6–9) is used only for the derivation of the physiologically meaningful parameters from moments. Each process occurring in this system is evaluated with statistical concepts of sum, mean, and variance, and the obtained parameters are free from restrictions arising from complex modeling. Thus, the moment analysis enables us to evaluate the disposition characteristics of drugs in the liver under various conditions.

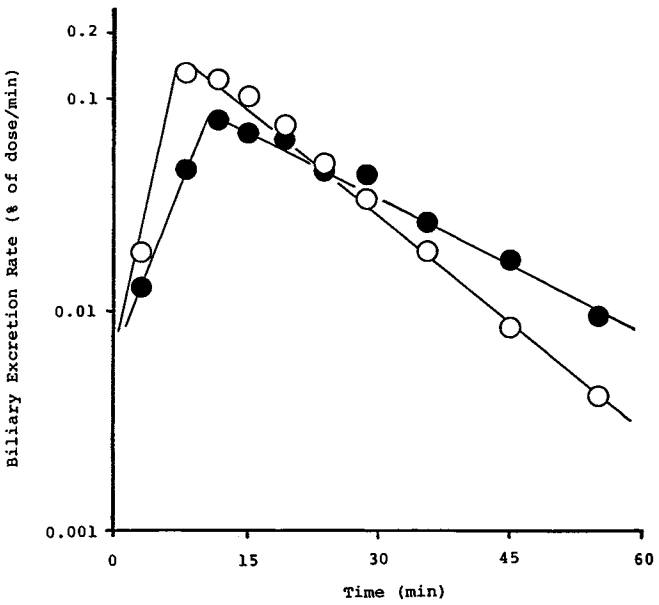

Fig. 5. Typical biliary excretion rate–time curves of free (○) and conjugated (●) phenol red at a dose of 1.33 mg/liver in the isolated rat liver perfusion system.

A concrete advantage of the present approach is that the assessment of drug disposition can be done dividing it into distribution and elimination processes. Furthermore, the elimination process can be evaluated with respect to rate and extent.

Moreover, we analyzed the biliary excretion of free and conjugated phenol red from the viewpoints of the two prior steps, namely, metabolism in the hepatocyte and secretion from the hepatocyte into the bile. These processes were characterized by the biliary recovery ratio ($F_{bile,free}$, $F_{bile,conj.}$) and biliary mean transit time ($\bar{t}_{bile,free}$, $\bar{t}_{bile,conj.}$)

The present investigation showed that the distribution volume of phenol red was about 123% (standard dose) of the original vascular space. This value seems to reflect the rapid phase of distribution between the vascular space and neighboring tissues.

The biliary mean transit times of free and conjugated phenol red were calculated to be 17.8 and 26.2 min, respectively (Table IV). These values indicate the time needed to move to the biliary sampling point from the inside of hepatocytes. The difference between $\bar{t}_{bile,free}$ and $\bar{t}_{bile,conj.}$ values (8.4 min) should correspond to the difference in secretion steps of free and conjugated phenol red and metabolism steps.

The data shown in Fig. 2 and Table II indicate that the hepatic disposition of phenol red obeys saturable kinetics. Generally, saturable kinetics are analyzed in terms of the Michaelis–Menten equation and quantified by the parameters of V_{max} and K_m (24,25). In the present approach, we assessed hepatic disposition by the parameters derived from moments ($k_{el,i}$, V_i, and $CL_{int,i}$). The value of $CL_{int,i}$ estimated in our method is equal to the intrinsic clearance obtained by ordinary methods (6–9) and would be utilized for Michaelis–Menten-type analysis. In addition, examination of the relationship between the dose and the V_i value would offer further information about the saturable kinetics of phenol red disposition from the viewpoint of distribution (uptake by hepatocytes). The total biliary recovery fraction of phenol red and recovery ratio of conjugated-to-free phenol red

Table IV. Moments for Biliary Excretion of Phenol Red (1.33 mg/Liver) in the Isolated Rat Liver Perfusion System (Values Are Means ± SD)

Condition	$F_{bile,free}$ (% of dose)	$F_{bile,conj.}$ (% of dose)	$\bar{t}_{bile,free}$ (min)	$\bar{t}_{bile,conj.}$ (min)	$F_{bile,conj.}/F_{bile,free}$
Standard dose, 37°C	1.80 ± 0.41	2.41 ± 0.62	17.8 ± 1.6	26.2 ± 1.9	1.34
High dose,[a] 37°C	0.89 ± 0.24*	0.89 ± 0.52*	13.6 ± 0.6*	17.8 ± 1.2*	1.00
Standard dose, 27°C	0.91 ± 0.21*	1.02 ± 0.59*	25.2 ± 5.2*	31.6 ± 4.5*	1.12

[a] The dose of phenol red was 4.00 mg/liver.
* $P < 0.05$ in comparison with the control (standard dose, 37°C).

(Table IV) also suggest the saturation kinetics in both transport and metabolism processes at the high dose.

In the case of low perfusion temperatures, V_i values of ^{131}I-HSA and phenol red increased significantly (Table III), suggesting an expansion of the actual liver vascular volume. A change in the liver vascular volume depending on the perfusion period was reported (26) but the present finding is another type of phenomenon. However, further discussion of the experimental data is not warranted. Although the absolute value of V_i for phenol red increased at low temperatures, the ratio of V_i values for phenol red to those for ^{131}I-HSA remained between 109 and 127% (Table III), suggesting that the distribution step was unaffected by temperature.

In spite of the large distribution volume (V_i), low temperatures resulted in decreased intrinsic clearance ($CL_{int,i}$) (Table III). The biliary recovery ratio of conjugated-to-free phenol red was significantly decreased, and the mean biliary transit time of free and conjugated phenol red was prolonged at low temperatures (Table IV). These data suggest that biliary excretion and metabolism of phenol red depend on temperature.

In conclusion, this experimental system is a useful method to evaluate the kinetics of hepatobiliary drugs transport. Moment analysis for local perfusion system was first applied to investigate drug disposition in the rabbit muscle (1), and disposition characteristics of various prodrugs were evaluated in relation to their physicochemical properties (27). The use of tumor-bearing tissue proved the wide applicability of statistical moment analysis (28). Further, since the moments are defined by transfer functions using Laplace transformation, network theory can also be applied to this analytical system. Hence, subsystems can be considered in parallel, and the effect of plasma protein binding on organ uptake was explored in our study (29). Another example is the deconvolution analysis of consecutive processes, which resulted in discrimination of several disposition parameters (30). The present study affords the first example of moment analysis applied to the evaluation of hepatobiliary transport of drugs.

ACKNOWLEDGMENT

This work was supported by a Grant-in-Aid for Scientific Research from the Ministry of Education, Science and Culture, Japan.

REFERENCES

1. T. Kakutani, K. Yamaoka, M. Hashida, and H. Sezaki. *J. Pharmacokinet. Biopharm.* 13:609–631 (1985).
2. G. E. Mortimore, F. Tietze, and D. Stetten. *Diabetes* 8:307–314 (1959).
3. L. G. Hart and L. S. Shanker. *Proc. Soc. Exp. Biol. Med.* 123:433–435 (1966).
4. K. Yamaoka, T. Nakagawa, and T. Uno. *J. Pharmacokinet. Biopharm.* 6:547–558 (1978).
5. D. J. Cutler, *J. Pharm. Pharmacol.* 30:476–478 (1978).
6. M. Rowland, L. Z. Benet, and G. G. Graham. *J. Pharmacokinet. Biopharm.* 1:123–136 (1973).
7. K. S. Pang and M. Rowland. *J. Pharmacokinet. Biopharm.* 5:625–653 (1977).
8. K. S. Pang and M. Rowland. *J. Pharmacokinet. Biopharm.* 5:655–680 (1977).
9. K. S. Pang and M. Rowland. *J. Pharmacokinet. Biopharm.* 5:681–699 (1977).
10. Y. R. Stollman, U. Gartner, L. Theilman, N. Ohmi, and A. W. Wolkoff. *J. Clin. Invest.* 72:718–723 (1983).
11. A. Blom, A. H. J. Scaf, and D. K. F. Meijer. *Biochem. Pharmacol.* 31:1553–1565 (1982).
12. R. Henry, B. Cueni, J. Bircher, and G. Paumgartner. *Naunyn-Schmiedeberg Arch. Pharmacol.* 277:297–304 (1973).
13. D. L. Gumucio, J. J. Gumucio, J. A. P. Wilson, C. Cutter, M. Krauss, R. Caldowell, and E. Chen. *Am. J. Physiol.* 246:G68–G95 (1984).
14. K. Takahashi, Y. Higashi, and N. Yata. *J. Pharmacobio-Dyn.* 9:570–577 (1986).
15. A. R. Fritzberg and J. Reichen. *J. Pharm. Pharmacol.* 37:919–922 (1985).
16. M. H. Finck, J. Reichen, J. M. Vierling, T. M. Kloppel, and W. R. Brown. *Am. J. Physiol.* 248:G450–G455 (1985).
17. C. A. Goresky and G. G. Bach. *Ann. N.Y. Acad. Sci.* 18:18–47 (1970).
18. J. B. Bassingthwaight. *Fed. Proc.* 41:3040–3044 (1982).
19. D. L. Yudilevich and G. E. Mann. *Fed. Proc.* 41:3045–3053 (1982).
20. M. Silverman and C. Trainor. *Fed. Proc.* 41:3054–3060 (1982).
21. M. S. Roberts and M. Rowland. *J. Pharmacokinet. Biopharm.* 14:227–260 (1986).
22. E. L. Forker and B. Luxon. *Am. J. Physiol.* 235:E648–E660 (1978).
23. R. A. Weisiger, C. M. Mendel, and R. R. Cavalieri. *J. Pharm. Sci.* 75:233–237 (1986).
24. B. F. Scharschmidt, J. G. Waggoner, and P. D. Berk. *J. Clin. Invest.* 56:1280–1292 (1975).
25. A. Blom, K. Keulemans, and D. K. F. Meijer. *Biochem. Pharmacol.* 30:1809–1816 (1981).
26. W. A. Dunn, D. A. Wall, and A. L. Hubbard. *Meth. Enzymol.* 98,225–241 (1983).
27. T. Kakutani, Y. Suematsu, W. Y. Cheah, E. Sumimoto, and M. Hashida. *Chem. Pharm. Bull.* 35:4898–4906 (1987).
28. R. Atsumi, K. Endo, T. Kakutani, Y. Takakura, M. Hashida, and H. Sezaki. *Cancer Res.* 47:5546–5551 (1987).
29. T. Kakutani, E. Sumimoto, and M. Hashida. *J. Pharmacokinet. Biopharm.* 16:129–149 (1988).
30. T. Kakutani, R. Atsumi, E. Sumimoto, and M. Hashida. *Chem. Pharm. Bull.* 35:4907–4914 (1987).